

# AN IMPROVED LATTICE FOR BTCF STORAGE RING

N. Huang, L. JIN, W. Liu, D. Wang, J. Wang, T. Wei, C. Yu  
IHEP, Chinese Academy of Sciences, P.O. box 918-9, Beijing 100039, P.R. of China

## Abstract

The latest study results of the lattice design of the Beijing Tau-Charm Factory (BTCF) are presented. Larger dynamic aperture of the high luminosity mode and higher luminosity with longer Touschek lifetime of the monochromator mode are achieved than the previous design. Some study of the spin matching of polarization mode is also included.

## 1 INTRODUCTION

In terms of the goals of the machine [1], the lattice is designed to take the high luminosity mode as the first priority, meantime to be compatible with the polarized beam collision mode and monochromator mode.

## 2 GENERAL DESCRIPTION

### 2.1 Considerations of Lattice Design

The key feature of lattice design is that it should have a high flexibility to accommodate the three modes mentioned above, i.e.

- The lattice can be adjusted to any of the three modes with the same layout of magnets.
- Beta functions at the interaction point (IP)  $\beta_x^*$  and  $\beta_y^*$ , nature emittance  $\epsilon_{x0}$ , tunes, etc., can be adjusted in a large range.
- The great flexibility in bunch number provides a possible enhancement of the luminosity.
- The large energy range with the potential up to 3 GeV is kept.

### 2.2 General layout of the ring

The BTCF consists of two rings, one above the other, with one interaction point (IP). The two rings are vertically separated about 1.67m. Each ring is 53m wide and 165m long with a circumference of 385.4m. It can be divided into four main parts: the interaction region (IR), two polarization insertions, two arcs and a utility region with injection section, as shown in Fig. 1. The main lattice parameters for the high luminosity mode and monochromator scheme are listed in Table 1.

## 3 HIGH LUMINOSITY MODE

The main challenge of this mode is how to get the luminosity of  $1 \times 10^{33} \text{ cm}^{-2} \text{ s}^{-1}$  at 2.0 GeV. The collision with a small horizontal crossing angle is chosen, because it is more capable of reaching the luminosity goal and offers the opportunity for great flexibility in the number of bunches

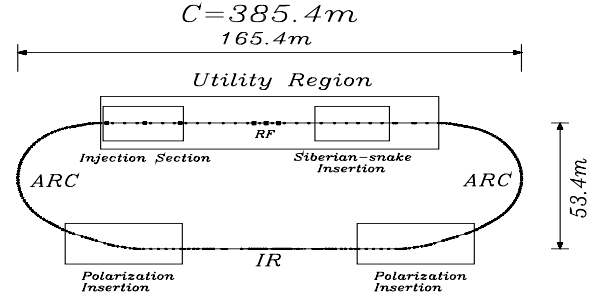


Figure 1: Schematic diagram of the BTCF storage ring

with the goal luminosity and possible enhancement of the luminosity. In addition, when the luminosity and the total beam current are determined, the large bunch number leads to a small current per bunch, a small natural emittance, a large threshold of impedance, a small momentum compaction factor, etc., which make the design parameters quite moderate and feasible.

The lattice functions of the whole ring for the high luminosity mode are shown in Fig. 2.

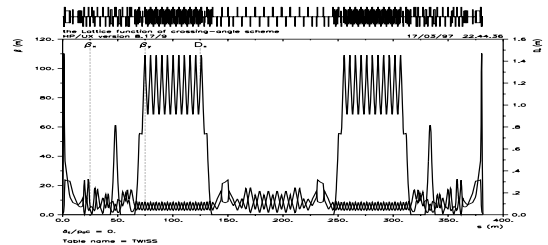


Figure 2: Twiss parameters of the high luminosity mode.

### 3.1 Interaction Region

At each side of the IP there are a micro-beta insertion and a vertical separation insertion. Fig. 3 shows the magnet layout in the region.

The two iron-free superconducting quadrupoles (Q1 and Q2) are used to achieve the micro-beta function at the IP. Q1 is 0.9 m away from the IP. The two beams are initially separated by an electrostatic separator ES with a length of 3.2m and the maximum ES field is limited below 1.5MV/m to avoid the risk of sparking due to a significant quantity of synchrotron radiation. The vertical offset quadrupole QV1 and three vertical bending septum magnets BV1, BV2 and BV3 further finish the beam separation. The bending angle

Table 1: Main lattice parameters of BTCF

Mode	High Lumi.	Mono.
Circumference (m)	385.4	385.4
Normal Energy (GeV)	2.0	1.55
Crossing angle at IP (mrad)	$2.6 \times 2$	0.0
Bending radius (m)	8.33	8.33
Beta-functions at IP (m)		
Hori./Vert.	0.66/0.01	0.01/0.15
Dispersion-functions at IP (m)		
Hori./Vert.	0.0/0.0	0.0/0.45
Natural horizontal emittance (nmrad)	138	83
Vertical emittance (nmrad)	2.1	5.3
Tunes, Hori./vert.	11.75/11.76	12.21/12.23
Natural chromaticities, H/V	-17/-35	-36/-31
Momentum compaction	0.014	0.014
Momentum spread ( $10^{-4}$ )	6	7.8(with wig.)
Damping time, H/V/Long. (ms)	30/30/15	26/61/90
Number of bunches	86	29
Particle per bunch ( $10^{10}$ )	5.4	9.3
Beam-beam parameters $\xi_x/\xi_y$	0.044/0.04	0.018/0.015
Luminosity ( $10^{33} \text{ cm}^{-2} \text{ s}^{-1}$ )	1.0	0.2
Energy spread at CM (MeV)	1.7	0.14

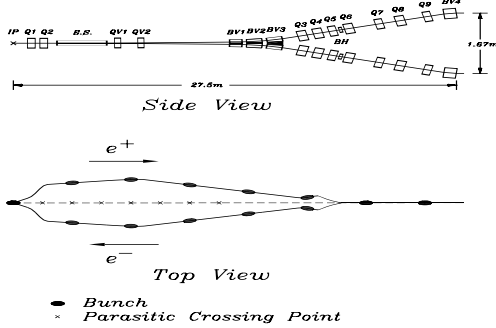


Figure 3: Magnet layout in IR region.

of BV3 is increased by 10mrad and the length of IR is 1m shorter than the previous design [2]. The last magnet BV4 brings the beam back to horizontal orbit. Six quadrupoles (Q3, Q4, Q6 to Q9) are arranged to finish focusing and vertical dispersion matching between BV3 and BV4. The maximum gradient of these quadrupoles is 15 T/m. The maximum vertical dispersion function is about 0.2 m in the region.

A pair of horizontal deflecting dipoles (BH), which are symmetrically placed just where the horizontal phase advance from the IP is  $\pi$ , produces a closed orbit distortion between the two BHs and makes the two beams collide at a small horizontal crossing angle (referred to the crossing angle scheme). When the BHs are turned off, head-on collisions can be obtained if necessary.

### 3.2 Polarization Insertion

The longitudinal polarization scheme adopted at around 1.84-2.0GeV in current BTCF design is symmetric

solenoid spin rotator. The rotator in each side of interaction region consists of three dipoles( two for spin rotation, one for compensation of bending angle adjustment), and two superconducting solenoids (9.63 T) which are switched off in high luminosity and monochromator modes, and many quadrupoles for the local coupling compensation and other matching. To reach an applicable polarization level, the spin-matching must be applied to suppress the strong depolarization effects even for the perfectly aligned machine. The spin-matching by adjusting 25 quadrupole strengths results in remarkable enhancement in depolarization time and equilibrium polarization level( 300 minutes and 80% respectively). Change in helicity can easily be achieved by reversing the field direction of the solenoid. The special design of the polarization mode has been described in ref.[3].

### 3.3 Arc

Each arc consists of 14 FODO cells, including 10 normal cells with  $60^\circ$  phase advance and one dispersion suppressor at each end of an arc. Each dispersion suppressor contains two FODO cells with wigglers instead of 2 normal bending magnets. But the wigglers are turn off in this mode. A special bending magnet with independent power supply is used in the dispersion suppressor near IR.

### 3.4 Utility Region

A long straight region lies on the side opposite to the IR. It consists of an injection insertion and four regular FODO cells and two beta-function matching sections as well. The kickers and Lambertson magnet are arranged in the injection insertion. The RF cavities are located in the regular cells which can provide over 3.2 m long drift spaces. The working points can be adjusted in this region.

### 3.5 Tracking Studies

The tracking and simulations ( without imperfections) are evaluated with the code MAD[5]. Except for the chromaticity sextupoles, no other correctors have been installed into the linear lattice. Simulations in six dimension are done for 2000 turns which corresponds to 1/12 damping time. Chromaticities in both transverse planes are corrected to a slightly positive value. Fig. 4 gives the tracking results of the high luminosity mode.

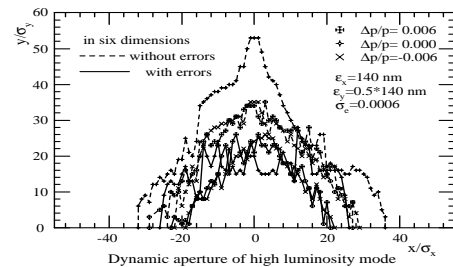


Figure 4: The dynamic aperture of the high lumi. mode

## 4 MONOCHROMATOR MODE

The aim of this mode is to get small spread of center-of-mass energy at the beam energy of 1.55 GeV. It will be realized by using opposite sign of vertical dispersion  $D_y^*$  for two beams at IP. The main challenge of this mode is how to get high luminosity and monochromatization factor with suitable Touschek lifetime[2].

### 4.1 IR region

The magnets layout in Fig. 3 keeps unchanged except the polarity of Q1, Q2, Q6 has to be changed, and Q4, Q8 and BHs are switched off. The lattice functions of this region are shown in Fig. 5. In order to increase luminosity the  $D_y^*$  value is changed from 0.35m to 0.45m comparing with the previous design[2].

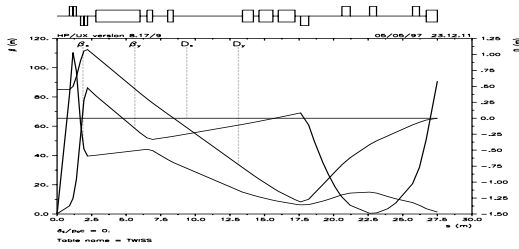


Figure 5: Lattice functions of the IR for the mono. mode.

### 4.2 Arc

The lattice of arc is similar to that of high luminosity mode except that eight Robinson wigglers in each ring are used for redistributing the damping partition number between  $J_x$  and  $J_e$  [4] so as to get low emittance. For this mode, the luminosity increases as the beam energy spread increases. When the Robinson wigglers decrease the emittance, it happens to increase the energy spread. The parameters of each Robinson wiggler (4 blocks) are chosen as the effective length of 0.84m (total length is 1.32m) with the dipole bending radius 14m and the gradient strength  $1.2m^{-2}$ ,  $J_x$  increases from 1 to 2.34 and  $J_e$  reduces from 2 to 0.66. As a result the emittance gets to about 36nmrad and the energy spread increases to  $8 \times 10^{-4}$  from the natural energy spread  $4.6 \times 10^{-4}$ . Fig. 6 shows the lattice functions in the arc.

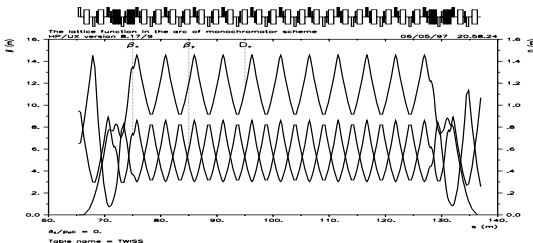


Figure 6: Lattice functions in arc for the mono. mode.

Table 2: Touschek lifetime of the monochromator mode

Energy acceptance $10^{-3}$	Emittance $x/y$ (nm)	Touschek lifetime hours
8	13/2	0.4
8	35/5.4	1.0
10	35/5.4	1.7
12	35/5.4	2.5
14	35/5.4	3.6

### 4.3 Touschek Lifetime

In order to increase the Touschek lifetime, large beam size and energy acceptance are necessary. So the normal cell with  $60^\circ$  phase advance is used in the arc to increase the dynamic aperture, energy acceptance and emittance ( $\epsilon_x=35$  nmrad with wigglers). The results calculated by the code ZAP[6] are shown in Table 2. The average Touschek lifetime is around 2 hours.

### 4.4 Dynamic Aperture

For the monochromator mode, 48 sextupoles of nine families are distributed in the arcs of each ring. The initial tracking results using the code MAD[5] in six dimensions with full coupling are shown as Fig. 7, that the dynamic aperture is  $18\sigma_x \times 18\sigma_y$  with  $\delta p = \pm 0.008$ .

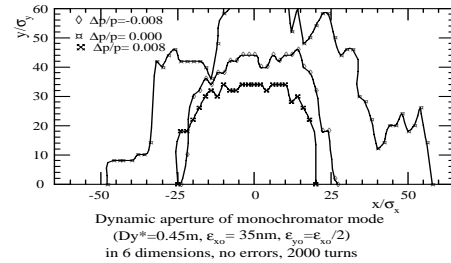


Figure 7: The dynamic aperture of the mono. mode.

## 5 CONCLUSION

The current lattice design is feasible to meet the requirements of the BTCF.

## 6 REFERENCES

- [1] Y.Z. Wu, Proceedings of Frascati'97 workshop.
- [2] "The Feasibility Report of Beijing Tau-Charm Factory", IHEP-BTCF, Report-03, October 1996
- [3] D. Wang, Proceedings of Frascati'97 workshop.
- [4] K. W. Robinson, "Radiation Effects in Circular Accelerator", Phys. Rev 111, 373 (1958)
- [5] H.Grote, F.C.Iselin, "The MAD Program", CERN/SL/90-13 (AP), 1990
- [6] M.S. Zisman, et al, "ZAP User's Manual", LBL-21270, 1986